applied sciences

MDPI

Article

Statistical Properties and Configurational Entropy of a Two-Dimensional Néel Magnetic Skyrmions Population

Roberto Zivieri

Department of Mathematical and Computer Sciences, Physical Sciences and Earth Sciences, University of Messina, 98166 Messina, Italy; zivieri@fe.infn.it

Received: 8 December 2019; Accepted: 29 December 2019; Published: 3 January 2020

Abstract: The study of the thermodynamic properties of topological defects is important not only for understanding their magnetic properties but also for suggesting novel applications. In this paper, the statistical and statistical thermodynamic properties of a population of Néel magnetic skyrmion diameters hosted in an ultrathin cylindrical dot is determined within a two-dimensional analytical approach. The statistical properties such as the skyrmion size are calculated in the region of skyrmion metastability and are compared with the ones obtained using a recent three-dimensional analytical approach based on the analogy with the Maxwell–Boltzmann distribution of dilute gas molecules. The investigations of the statistical thermodynamic properties focus on the calculation of the configurational entropy at thermodynamic equilibrium determined in the continuous limit from the Boltzmann order function. While the statistical properties are quantitatively similar passing from the two-dimensional to the three-dimensional approach, the configurational entropy calculated from the two-dimensional skyrmions distribution is considerably lower than the one obtained from the three-dimensional skyrmions distribution. Because of the strong resemblance between the statistical configurational entropy and Jaynes's information entropy, it is suggested to use magnetic skyrmions as temperature and external field dependent information entropy carriers for a future potential technological application in the field of low-dimensional magnetic systems and skyrmionics.

Keywords: topological defects; low-dimensional magnetic systems; magnetic skyrmions; configurational entropy; two-dimensional skyrmion diameters distribution; three-dimensional skyrmion diameters distribution; Shannon's information entropy; information entropy carriers

1. Introduction

Magnetic skyrmions are axisymmetric topological solitons hosted in ferromagnetic materials (see [1,2] and references therein) stabilized by the Dzyaloshinskii–Moriya interaction (DMI), a relativistic exchange interaction [3,4]. Magnetic skyrmions are characterized by a skyrmion number (otherwise called topological charge) $S = 1/(4\pi) \int \mathrm{d}^2\rho\ \mathbf{m}\cdot(\partial\mathbf{m}/\partial x \times \partial\mathbf{m}/\partial y)$ where $\mathbf{m}(\rho) = \mathbf{M}(\rho)/M_s$ is the unit magnetization vector with $\mathbf{M}$ the magnetization, $\rho = (x, y)$, and M_s the saturation magnetization, and $\partial/\partial x$ and $\partial/\partial y$ are first partial derivatives.

There are two types of DMI, the interfacial DMI (IDMI) stabilizing chiral Néel (hedgehog-like) and the bulk DMI stabilizing Bloch (vortex-like) skyrmions. In early 2000, Bogdanov and Rößler developed a phenomenological theory of chiral symmetry breaking in magnetic thin films and multilayers, and they predicted the formation of skyrmions in magnetic thin films and multilayers stabilized by induced DMI interactions [5]. Afterwards, it has been theoretically demonstrated that skyrmion structures can be formed as spontaneous ground states in magnetic metals with DMI interactions without the need of applying external fields or the presence of defects [6].

Recently, several efforts were done to study static properties, such as skyrmion stability in low-dimensional magnetic systems [7], and dynamic properties (see e.g., [8,9]). However, until recently, not much attention has been paid to the investigation of statistical and statistical thermodynamic properties of magnetic skyrmions. In particular, only during the last years the problem of entropy for magnetic skyrmions was faced. The skyrmion entropy has been estimated from experimental data and its thermodynamic meaning has been used in bulk B20 compounds to give a classification of the magnetization phase transition at the transition temperature [10,11]. Its inclusion in the Arrhenius law turned out to be determinant to explain the disagreement between the measurement and the calculation of the lifetime of a skyrmion lattice [12]. In a recent paper, the configurational entropy of a skyrmion diameters population was calculated within a three-dimensional (3D) approach showing that the entropy can be expressed as a function of physical and geometrical parameters and temperature. According to the 3D model, the distribution of the skyrmion diameters population represents the analogous of the Maxwell–Boltzmann (MB) distribution of particles for a dilute ideal gas and, on this basis, the configurational entropy, thermal fluctuations of energy and the statistical thermodynamics of chiral skyrmions were investigated (see [13,14] and references therein). As observed in micromagnetic simulations [13], configurational entropy can be regarded as the number of different skyrmions having the same average energy resulting from the thermal fluctuations that enable the promotion of a number of skyrmions possessing the same average energy. In the 3D analytical model, it was expressed as a quantity proportional to $<\ln f_0>$ where $< \dots >$ denotes the statistical average over the spatial coordinates and f_0 is the Gaussian distribution of diameters at thermodynamic equilibrium depending on the skyrmion diameter D_{sky} and on its average value.

Instead, in the present work the skyrmions population is regarded as a two-dimensional (2D) distribution considering that skyrmions are planar structures. From this point of view, the analogy with the ideal gas is not so strict because the 2D distribution is not, strictly speaking, the direct correspondent of the ideal gas MB distribution. However, the analogy can be considered still valid because the 2D skyrmion diameters distribution can be written in a form proportional to a Gaussian distribution in turn depending on the skyrmion energy and, as a result, the configurational entropy can be expressed as a quantity proportional to $<\ln f_0>$.

The aim of this paper is to determine, by means of a simple analytical model, the statistical and statistical thermodynamic properties of a 2D Néel skyrmion diameters distribution. The statistical properties are related to the calculation of the 2D skyrmion diameters distributions, of the most probable and average diameters and of standard deviations of the 2D distributions as a function of temperature T. The average diameters and standard deviations, obtained within the 2D model, are compared with the ones determined within the 3D model. Regarding the statistical thermodynamic properties, the analysis focuses on the calculation of the configurational entropy as a function of the temperature T and of the external bias field in a 2D framework. This is accomplished investigating the static behavior of a skyrmions population hosted in a ferromagnetic material (e.g., Co) that has the shape of an ultrathin cylindrical dot starting from the skyrmion energy evaluated as a function of the skyrmion diameter in the region of skyrmion metastability [15]. The configurational entropy, calculated according to the 2D model, is then compared with the one obtained via the 3D model and the quantitative differences are discussed. Additionally, as in the 3D model, it is crucial, for characterizing in a quantitative way the 2D distribution, the knowledge of the average diameter, a key quantity appearing in the configurational entropy.

It is found that the properties related to the size of skyrmions and the statistical distribution of skyrmion diameters do not essentially depend on the dimensionality of the problem (either 2D or 3D) and the results are very similar in the region of skyrmion metastability. On the other hand, while qualitatively the behavior of the configurational entropy as a function of the temperature is similar, the configurational entropy computed within the 2D approach is considerably smaller than that calculated within the 3D approach. This discrepancy is attributed to the different dependence on the temperature T of the configurational entropy passing from the 2D to the 3D description and to the role of the

thickness of the magnetic skyrmions appearing in the 3D configurational entropy. Moreover, it is found that, within the 2D model, the configurational entropy does not exhibit anymore a decreasing monotonic behavior as a function of the external bias field. According to these results, even though skyrmions are planar structures, the 3D description of a skyrmions population is preferable.

It is also given a qualitative description of an entropy data communication system that could be used for a possible future application of the present thermodynamic analysis suggesting the use of skyrmions as temperature and field dependent information entropy carriers. This is based on the complete identification between the configurational entropy at thermodynamic equilibrium calculated here and Jaynes continuous version of discrete Shannon's information entropy [16–26].

In this respect, very recently, the configurational entropy in 2D skyrmion-like and vortex-like configurations has been investigated for different forms of topological charge density [27] and as a measure of ordering in field configuration space for nonlinear models with spatially-localized energy solutions [28]. Finally, note also that, in the recent literature, there are several papers dealing with the employment of magnetic skyrmions as information carriers but according to completely different approaches based on the skyrmion state and not on the skyrmion entropy (see e.g., [29–32]).

The paper is organized as follows. In Section 2 the analytical model for the calculation of the 2D configurational entropy of a Néel skyrmion is outlined. In Section 3 the numerical results are presented and discussed. Section 4 gives a qualitative description of an information system for a future application. In Section 5 conclusions are drawn.

2. Analytical Model

In this section, the analytical model for the calculation of the configurational entropy for a 2D Néel skyrmion diameters distribution is outlined. It is briefly recalled the computation of the skyrmion energy and then the 2D distribution is introduced to calculate the most probable diameter, the average diameter, the standard deviation and the 2D configurational entropy from the Boltzmann order function at thermodynamic equilibrium.

2.1. Skyrmion Energy

It has been considered an outwardly directed radial Néel skyrmion with a magnetization pointing along $-z$ at the core center (skyrmion number $S = -1$) stabilized in an ultrathin magnetic cylindrical dot of radius R_d in a cylindrical reference frame (ρ, φ, z) with ρ the radial coordinate, φ the azimuthal coordinate and z the coordinate perpendicular to the dot plane. Néel skyrmion's texture, expressing the orientation of the magnetization, is $\mathbf{m}(x, y) = \sin\theta(\rho)\hat{\rho} + \cos\theta(\rho)\hat{z}$ with $\mathbf{m} = \mathbf{M}/M_s$, $\mathbf{m} = (m_\rho, m_z)$ and θ the polar angle. In Figure 1, a pictorial representation of the ferromagnetic cylindrical dot (e.g., Co) hosting the Néel magnetic skyrmion is shown together with the cylindrical reference frame. The skyrmion has a cylindrical symmetry with respect to the out-of-plane direction (z-axis). The cylindrical dot is assumed to be in contact with a thin layer of heavy metal (e.g., Pt) providing a consistent IDMI interaction (not shown).

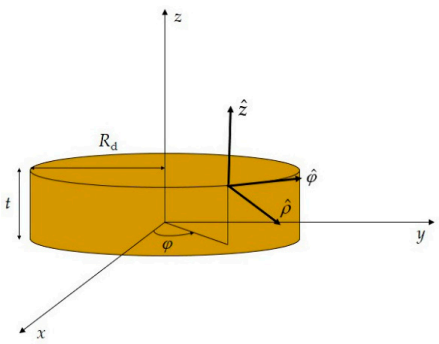

Figure 1. A sketch of the cylindrical dot hosting the Néel skyrmion with R_d the dot radius and t the dot thickness. A cylindrical reference frame (ρ, φ, z) is also shown.

The skyrmion energy E was numerically calculated as a volume integral of the skyrmion energy density ε_{tot}, namely $E\left(r_{\text{sky}}\right) = \int \varepsilon_{\text{tot}}\left(r, r_{\text{sky}}\right) dV = \int_{-t/2}^{t/2} dz \int_{0}^{2\pi} d\varphi \int_{0}^{R_d} \varepsilon_{\text{tot}}\left(r, r_{\text{sky}}\right) \rho d\rho$. Here, t is the dot thickness, $r_{\text{sky}} = R_{\text{sky}}/l_{\text{exch}}$ is the dimensionless skyrmion radius with R_{sky} the skyrmion radius and $l_{\text{exch}} = \sqrt{2A/(\mu_0 {M_{\text{s}}}^2)}$ the exchange length being μ_0 the vacuum permeability. For the skyrmion energy calculation it has been used as the ansatz distribution $\Theta_0(r) = 2\arctan[\frac{B}{r} e^{-\xi r}]$ expressing the magnetization at equilibrium in excellent agreement with the magnetization distribution of micromagnetic simulations [15]. Here, $B = r_{\text{sky}} \exp[\xi\, r_{\text{sky}}]$ being $\xi = \sqrt{Q} - 1$ ($Q = 2K_{\text{u}}/(\mu_0 {M_{\text{s}}}^2)$ is the quality factor with K_{u} the uniaxial anisotropy constant), $r_{\text{sky}} = R_{\text{sky}}/l_{\text{exch}}$ is the dimensionless skyrmion radius and $r = \rho/l_{\text{exch}}$ is the dimensionless radial coordinate. The skyrmion energy density $\varepsilon = \varepsilon_{\text{exch}} + \varepsilon_{\text{IDMI}} + \varepsilon_{\text{ani}} + \varepsilon_{\text{ext}}$ contains all the relevant contributions. In particular, $\varepsilon_{\text{exch}} = A(\nabla \mathbf{m})^2$ is the exchange energy density with A the material exchange stiffness constant, $\varepsilon_{\text{IDMI}} = D\,[m_z(\nabla \cdot \mathbf{m}) - (\mathbf{m} \cdot \nabla) m_z]$ is IDMI energy density with D the DMI parameter, $\varepsilon_{\text{ani}} = K_{\text{u}}\left(1 - m_z^2\right) + \frac{1}{2}\mu_0 M_s^2 m_z^2$ is the anisotropy energy density including the perpendicular uniaxial anisotropy energy density and the magnetostatic energy density in the ultrathin approximation, and $\varepsilon_{\text{ext}} = -M_{\text{s}}\, B_{\text{ext}}\, m_z$ is the Zeeman energy density with $B_{\text{ext}} = \mu_0 H_{\text{ext}}$ the amplitude of the external bias field parallel to the z-axis. The computation of the 2D configurational entropy is based on the calculation of the skyrmion energy. Details about the numerical calculation of the skyrmion energy can be found in [13,14].

As done for the 3D model, the main hypothesis allowing a simplification of the calculation of the configurational entropy is the harmonic approximation. This approximation consists of modelling the skyrmion energy via a parabolic potential $E \approx a\,(D_{\text{sky}} - D_{0\,\text{sky}})^2 + b$. Here, the coefficient a is proportional to the parabola curvature, $a = \frac{1}{2} d^2E/d{D_{\text{sky}}}^2$, with $0 \le D_{\text{sky}} \le 2R_{\text{d}}$ and $D_{0\,\text{sky}} = D_{0\,\text{sky}}\,(T)$ the equilibrium skyrmion diameter in correspondence of which the energy attains a minimum E^{min} for every T, and the coefficient $b = E^{\text{min}}$ gives the translation of the energy minimum with respect to the zero energy and does not depend on D_{sky}. Note that the contribution of E depending on b is at least three orders of magnitude larger than the average contribution proportional to a for the used magnetic parameters but, because it does not depend explicitly on D_{sky}, it is not included in the calculation of the configurational entropy. $D_{0\,\text{sky}}$ depends on the temperature via the scaled values of the magnetic parameters; therefore, both a and b are temperature-dependent coefficients, $a\,(T)$ and $b(T)$.

2.2. Statistical and Thermodynamic Properties of the Skyrmion Diameters Population

In this section, the statistical and statistical thermodynamic properties of the skyrmion diameters population are described for the 2D model and compared to those of the 3D model. In particular, the skyrmion size is determined by calculating skyrmion diameters and the standard deviations of the distributions as a function of T. Regarding the thermodynamic properties, the configurational entropy within the 2D model is computed as a function of T and, at fixed T, as a function of the external bias field and compared to that of the 3D model.

2.2.1. Skyrmion Diameters Distribution

The 3D approach within which, as a first approximation, the skyrmion energy was well-described by a quadratic function of the skyrmion diameter has led to the hypothesis that the skyrmion diameters distribution can be treated as the particles of an ideal gas, at least from a statistical thermodynamics viewpoint. Therefore, the population of the skyrmion diameters was supposed to follow a MB distribution function.

Note that, strictly speaking, the MB distribution at thermodynamic equilibrium that describes the statistical behavior of an ideal gas, obtained ignoring interactions and correlations among the particles, is provided exactly by a canonical ensemble. A canonical ensemble is a statistical ensemble whose corresponding system exchanges energy with a thermal bath leading to states having different energies and thus subject to thermal fluctuations of energy varying with time. However, in the thermodynamic limit (number of particles $N \to \infty$) implying volume $V \to \infty$ and realized for the case of an ideal gas for

$N = N_A$ with $N_A = 6.02 \times 10^{23}$ the Avogadro number, the MB distribution can be provided also by a microcanonical ensemble. This statistical ensemble is characterized by microscopic states having a well-defined energy whose thermal fluctuations are very small if compared to the average energy to be considered negligible. For the present case the 3D MB distribution of skyrmion diameters, with no interactions and correlations one with each other, can be written within a microcanonical ensemble, analogously to the 3D MB of an ideal gas, as [13]:

$$\frac{dn_{3D}}{dD_{sky}} = C^{3D}_{sky\,0} D^2_{sky} e^{-\frac{a}{k_B T}(D_{sky} - D_{0\,sky})^2} \quad (1)$$

where dn is the number of times one gets a skyrmion diameter between D_{sky} and $D_{sky} + dD_{sky}$, $C^{3D}_{sky\,0}$ is the normalization constant of the 3D distribution and $k_B = 1.38 \times 10^{-23}$ J/K is the Boltzmann constant. Passing from a 3D to a 2D description the analogy with the ideal gas becomes weaker because of the different dimensionality. Nonetheless, without loss of generality, it is still possible to define the corresponding 2D distribution of skyrmion diameters as proportional to the equilibrium Gaussian distribution centered at the equilibrium skyrmion diameter $D_{0\,sky} = D_{0sky}(T)$ in the form:

$$\frac{dn_{2D}}{dD_{sky}} = C^{2D}_{sky\,0} D_{sky} e^{-\frac{a}{k_B T}(D_{sky} - D_{0\,sky})^2} \quad (2)$$

where $C^{2D}_{sky\,0}$ is the normalization constant of the 2D distribution. By comparing Equation (1) with Equation (2), one notes that the equilibrium Gaussian distribution has the same form because it depends on the skyrmion energy in the harmonic approximation. However, the 2D skyrmion distribution of Equation (2) is proportional to D_{sky} and not to D^2_{sky} as for the 3D distribution taking into account that one deals with a planar structure depending on the in plane coordinates only. From the minimization of Equation (1), it was found that the displacement law as a function of the temperature of the diameters distribution in the 3D model reads [13]:

$$D^{mp\,3D}_{sky}(T) = \frac{1}{2} D_{0\,sky}\left(1 + \sqrt{1 + \frac{4k_B T}{a\, D^2_{0\,sky}}}\right). \quad (3)$$

Analogously, from the minimization of Equation (2), the corresponding displacement law as a function of the temperature of the diameters distribution in the 2D model is:

$$D^{mp\,2D}_{sky}(T) = \frac{1}{2} D_{0\,sky}\left(1 + \sqrt{1 + \frac{2k_B T}{a\, D^2_{0\,sky}}}\right). \quad (4)$$

Here, the superscript "mp" stands for "most probable" and $D^{mp\,2D}_{sky}(T)$ is the most probable value of the skyrmion diameter for the 2D model. This value represents the skyrmion diameter corresponding to the maximum of the 2D skyrmion distribution. Equation (4) can be regarded as the law of displacement of the maximum of the 2D skyrmions distribution. This law expresses the displacement of the maximum of the distribution as a function of T. As for the 3D model, a displacement effect of the maximum of the distribution occurs because the skyrmion energy is comparable with the thermal energy.

The most probable diameter depends on the equilibrium diameter $D_{0sky}(T)$ at a given T but has also a dependence on the ratio between the thermal energy $k_B T$ and the skyrmion energy $a\, D^2_{0sky}$ in correspondence of the equilibrium diameter. As in the range of temperatures 50 ÷ 300 K $k_B T$ is comparable to $a\, D^2_{0sky} D_{0sky}{}^2$ (indeed, $k_B T$ is on average one order of magnitude less than $a\, D^2_{0sky}$ and not much smaller), there is a noticeable displacement of the maximum of the distribution as a function

of T. At low temperatures, $D^{mp}_{sky}(T)$ expanded to the first-order in T has a linear dependence on T assuming that $D_{0sky}(T) = D_{0sky}\ (T = 0\ \mathrm{K}) + d\ T$ with d a coefficient expressed in m/K.

2.2.2. Average Skyrmion Diameter

The average skyrmion diameter at a given temperature T for a skyrmion diameters population is obtained by integrating D_{sky} over the 2D diameters distribution and normalizing:

$$< D^{2D}_{sky}(T) > \ = \ \frac{\int_0^\infty dD_{sky} D^2_{sky} e^{-\frac{a}{k_B T}\ (D_{sky} - D_{0\ sky})^2}}{\int_0^\infty dD_{sky} D_{sky} e^{-\frac{a}{k_B T}\ (D_{sky} - D_{0\ sky})^2}}. \tag{5}$$

The result of the integration is:

$$< D^{2D}_{sky}(T) > \simeq D_{0\ sky}\left(1 + \frac{k_B T}{2a\, D^2_{0\ sky}}\right). \tag{6}$$

In particular, in the limit for $T \to 0$ K it is $< D_{sky}(T \to 0\ \mathrm{K}) > \ = \ D_{0\ sky}(T \to 0\ \mathrm{K})$ as in the 3D model. Equation (6) is different from the one found in [13] according to the 3D approach that reads:

$$< D^{3D}_{sky}(T) > \simeq D_{0\ sky}\left(\frac{3\, k_B T + 2a\, D^2_{0\ sky}}{k_B T + 2a\, D^2_{0\ sky}}\right). \tag{7}$$

2.2.3. Standard Deviation of the Skyrmion Diameters Distribution

In order to have a quantitative measure of the distribution it is crucial to compute the standard deviation $\sigma^{2D}_{<D^{2D}_{sky}>}$ of the 2D diameters distribution. The standard deviation is expressed as a normalized integral over the 2D diameters distribution at a given temperature and external bias field of the square deviation from the average diameter:

$$\sigma^{2D}_{<D^{2D}_{sky}>} \ = \ \left[\frac{\int_0^\infty dD_{sky}\left(D_{sky} - < D^{2D}_{sky} >\right)^2 D_{sky}\, e^{-\frac{a}{k_B T}\ (D_{sky} - <D^{2D}_{sky}>)^2}}{\int_0^\infty dD_{sky} D_{sky}\, e^{-\frac{a}{k_B T}\ (D_{sky} - <D^{2D}_{sky}>)^2}}\right]^{\frac{1}{2}} \tag{8}$$

The result of the integration is:

$$\sigma^{2D}_{<D^{2D}_{sky}>}(T) \ = \ \sqrt{\frac{k_B T}{2a}}. \tag{9}$$

This expression differs from the standard deviation determined according to the 3D approach where there is, in addition, also an explicit dependence of $\sigma^{3D}_{<D_{sky}>}(T)$ on the average skyrmion diameter. For a comparison, $\sigma^{3D}_{<D_{sky}>}(T)$ reads [13]:

$$\sigma^{3D}_{<D^{3D}_{sky}>}(T) \ = \ \sqrt{\frac{k_B T}{2a}\left(\frac{3 k_B T + 2\, a\ < D^{3D}_{sky} >^2}{k_B T + 2\, a\ < D^{3D}_{sky} >^2}\right)}. \tag{10}$$

However, as shown in Section 3, this additional dependence does not essentially affect the trend of the standard deviation within the 3D model that has values close to those exhibited according to the 2D model.

2.2.4. Configurational Entropy of Skyrmion Diameters Distribution

The average diameter of the skyrmion diameters distribution is a key quantity for the computation of the corresponding skyrmion configurational entropy within the 2D approach analogously to what occurred according to the 3D approach. Note that, also in this case, the source of entropy is mainly due to the skyrmion internal deformations and thermal breathing mode.

Even though the analogy with the dilute ideal gas is not so strong as in the 3D approach due to the different dimensionality, it is still reasonable to define the 2D Boltzmann order function ${H_0}^{2D}$ at thermodynamic equilibrium recalling its 3D definition for a dilute ideal gas in the continuous limit, exact solution of Boltzmann's kinetic equation at thermodynamic equilibrium as defined by Boltzmann's *H*-theorem. The passage from the discrete to the continuous is justified by the fact that the changes of the skyrmion size along the radial direction are very small as was observed in micromagnetic simulations [15]. H_0 represents a measure of order and, within the 2D approach, is still proportional to the Gaussian skyrmion diameters distribution. Specifically, H_0 is the opposite of the entropy S at equilibrium, namely $H_0 = -S/k_{B,}$ with $H_0 < 0$. In the continuous case applied to this framework, taking into account the 2D cylindrical symmetry, H_0^{2D} is written as a functional integral over the in-plane cylindrical coordinates, viz:

$$H_0^{2D} = \pi \int_0^{\infty} dD_{sky} D_{sky} f_0 \ln f_0. \quad (11)$$

H_0^{2D} represents the statistical average $<\ln f_0>$ with $f_0 = C_{sky}^{av2D} e^{-\frac{a}{k_B T}(D_{sky} - <D_{sky}^{2D}>)^2}$ the Gaussian distribution of the skyrmion diameters centered at the average diameter $< D_{sky}^{2D} >$ at thermodynamic equilibrium or probability density function where C_{sky}^{av2D} is the normalization constant of the 2D distribution (the superscript "av" denotes average). Here, the azimuthal angular dependence is given by π instead of 2π because D_{sky} is considered in place of the skyrmion radius R_{sky}. This 2D distribution has the meaning of a probability density at equilibrium in statistical mechanics as occurs for the 3D distribution. The 3D equivalent is [13]:

$$H_0^{3D} = 2\pi \int_0^{\infty} dD_{sky} D_{sky}^2 f_0 \ln f_0 \quad (12)$$

where $f_0 = C_{sky}^{av3D} e^{-\frac{a}{k_B T}(D_{sky} - <D_{sky}^{3D}>)^2}$. The computation of the integral of Equation (11), via the substitutions $f_0 = C_{sky}^{av2D} e^{-\frac{a}{k_B T}(D_{sky} - <D_{sky}^{2D}>)^2}$ and $\ln (C_{sky}^{av2D}) \rightarrow \ln (C_{sky}^{av2D} A_{sky})$ performed for dimensional reasons with $A_{sky} \approx \frac{1}{4}\pi <{D_{sky}}^{2D}>^2$ the average area of the skyrmion surface at a given T, yields:

$$H_0^{2D} = C_{sky}^{av2D} \pi^{\frac{3}{2}} \left(\frac{k_B T}{a}\right)^{\frac{1}{2}} < D_{sky}^{2D} > \left[\ln\left(C_{sky}^{2D} A_s\right) - \frac{1}{2}\right]. \quad (13)$$

C_{sky}^{av2D} has the dimension of an inverse of an area and is determined by means of the normalization condition $C_{sky}^{av2D} = \frac{1}{\pi}\left[\int_0^{\infty} dD_{sky} D_{sky} \; e^{-\frac{a}{k_B T}(D_{sky} - <D_{sky}^{2D}>)^2}\right]^{-1}$ (note that the definition of C_{sky}^{av2D} depends on $< D_{sky}^{2D} >$ and is slightly different from the one of $C_{sky\,0}^{2D}$ that depends on $D_{0\,sky}$). This condition is obtained via the normalization to unity (in place of the normalization to the particles density

$n = N/V$ for ideal gas) resulting in $C_{sky}^{av2D} = \frac{1}{\pi^{\frac{3}{2}}}\left(\frac{a}{k_B T}\right)^{\frac{1}{2}} \frac{1}{<D_{sky}^{2D}>}$. Substituting C_{sky}^{av2D} and A_s into H_0^{2D} of Equation (13) yields:

$$H_0^{2D} = -\frac{1}{2}\left(\ln\left(\frac{16\,\pi k_B T}{a\ <D_{sky}^{2D}>^2}\right)+1\right). \quad (14)$$

The configurational skyrmion entropy of the 2D skyrmions population at thermodynamic equilibrium is calculated as $S = -k_B\, H_0$:

$$S^{2D}(T) = \frac{1}{2}k_B\ \ln\left(\frac{16\,\pi\, k_B T}{a\ <D_{sky}^{2D}>^2}\right)+S_0 \quad (15)$$

with $S_0 = 1/2k_B$ and $< D_{sky}^{2D} >$ calculated by means of Equation (6). S^{2D} exhibits a logarithmic dependence and the logarithm argument depends on the ratio between the thermal energy $k_B T$ and the average skyrmion energy $a\ <D_{sky}^{2D}>^2$. For a comparison, the corresponding configurational entropy computed in [13] for the 3D skyrmion diameters population reads:

$$S^{3D}(T) = k_B\left[\ln\left(\frac{(k_B T)^{\frac{3}{2}}+2(k_B T)^{\frac{1}{2}}a\ <D_{sky}^{3D}>^2}{a^{\frac{3}{2}}\ <D_{sky}^{3D}>^2\ t}\right)+\frac{1}{2}\left(\frac{3k_B T+2a\ <D_{sky}^{3D}>^2}{k_B T+2a\ <D_{sky}^{3D}>^2}\right)\right]+S_0 \quad (16)$$

with $S_0 = k_B\ (2\ln 2 + 1/2 \ln \pi)$. Looking at Equation (15) one notes that, as within the 3D model (Equation (16)), the configurational entropy has a geometric, thermal, and magnetic parameters dependence. However, while S^{3D} includes a logarithmic contribution and a fractional contribution having different dependences on T, S^{2D} is proportional only to a logarithmic contribution and has no explicit dependence on the thickness t of the ferromagnetic material hosting the skyrmion. This results in a configurational entropy that is much smaller than the one calculated according to the 3D model. This difference highlights also the role played by the thickness t of the magnetic skyrmion (see Equation (16)) in the 3D model. In both cases, the configurational entropy depends on the size of the skyrmion via the average skyrmion diameter, has a dependence on the thermal energy even though with different functional forms decreasing with decreasing temperature, and is affected by the magnetic parameters by means of the coefficient a. The dependence on the skyrmion size in both the 2D and 3D frameworks confirms the link with the skyrmion breathing mode independently of the considered dimensionality. As for S^{3D} the thermal dependence becomes critical below $T = 1$ K because S^{2D} diverges negatively violating Nernst's third principle of thermodynamics (see the next subsection for more details). Finally, also S^{2D} expressed in Equation (15) can be considered a general result because other skyrmion textures would lead to energy profiles that can be approximated via the harmonic approximation in the vicinity of their minimum.

2.2.5. Behavior of $<D_{sky}{}^{2D}>$, $\sigma_{Dsky}{}^{2D}$, and S^{2D} at Low Temperatures

It is interesting to derive the low-temperature behavior ($0 \div 50$ K) of the average skyrmion diameter, the standard deviation and the configurational entropy [13]. The low-temperature relations obtained are still classical because they are based on relations derived within the classical 2D distribution of diameters at equilibrium. For the whole range of temperatures studied ($0 \div 300$ K) and for each external bias field, $a(T) = a_0 + c\,T$ with $a_0 = a\ (T = 0$ K) and $c < 0$ a coefficient expressed in J/(m^{2}K) [13]. Moreover, at low temperatures, $D_{0sky}\ (T) = D_{0sky}\ (T = 0\ \text{K}) + d\,T$. It has been found from numerical calculations that $<D_{sky}\ (T \to 0\ \text{K})> = D_{0sky}\ (T \to 0\ \text{K})$ as occurred for the 3D distribution (strictly speaking, it is indeed

not possible to define an average diameter for $T = 0$ K). Hence, at low temperatures, the expansion of Equation (6) to the first-order yields:

$$< D^{2D}_{sky}(T) >_{T\to 0\ K} \simeq D^{\ 0}_{0\ sky}\left(1 + \frac{k_B T}{2\,a_0\left(D^{\ 0}_{0\,sky}\right)^2}\right) \tag{17}$$

with $D^{0}_{0\ sky} = D_{0sky}$ ($T = 0$ K) for every amplitude of the external bias field. This expression is similar to Equation (6) but note that $a(T)$ is replaced by a_0 and D_{0sky} by $D^{0}_{0\ sky}$. This leads to a purely linear dependence of the skyrmion average diameter on T at low temperatures at fixed a_0 and $D^{0}_{0\ sky}$.

At low temperatures ($T\to 0$ K), via a series expansion to the first-order of Equation (9), writing $a = a_0 + c\,T$, the standard deviation turns out to be:

$$\sigma^{2D}_{<D^{2D}_{sky}>}(T)_{(T\to 0\,K)} \simeq \sqrt{\frac{k_B T}{2a_0}}. \tag{18}$$

Hence, at low temperatures, the standard deviation has a square root proportionality on temperature. In the same way, the configurational entropy S^{2D} of Equation (15) expanded to the first-order at low temperatures (for $T\to 0$ K), via Equation (17), reads:

$$S^{2D}(T)_{(T\to 0\,K)} \simeq \frac{1}{2}k_B\left(\ln\left(\frac{16\,\pi\,k_B T}{a_0\left(D^{\ 0}_{0\,sky}\right)^2}\right) - \frac{c\,T}{a_0}\right) + S_0 \tag{19}$$

neglecting the small term $-\frac{1}{2}\frac{k_B^2\,T}{a_0\left(D^{\ 0}_{0sky}\right)^2}$ resulting from the low-temperature expansion of the average diameter.

The first term on the second member has a logarithmic dependence on T, hence giving the divergence of S for $T = 0$ K. On the other hand, the second term expresses the linear dependence of S on T and vanishes for $T = 0$ K. As occurred for S^{3D}, at low temperatures there is a deviation from the linear behavior due to the logarithmic dependence on T of the first term. The passage from the 3D to the 2D description does not avoid the unphysical divergent result as $T\to 0$ K. This confirms that this result does not depend on the dimensionality but on the fact that the configurational entropy was computed according to a classical approach showing the same limits of the Sackur–Tetrode entropy equation for the ideal gas and that, as $T\to 0$ K, a quantum approach would be necessary to remove the divergent behavior. Numerically, analogously to the 3D model, the calculations performed according to Equations (6), (9) and (15) for the average diameter, the standard deviation and the configurational entropy, respectively, within the 2D model are well reproduced by the corresponding low-temperature expansions to the first-order of Equations (17)–(19), respectively for 1 K $\le T \le$ 50 K. The curve of $< D^{2D}_{sky}(T) >_{T\to 0\ K}$ is almost superimposed to that of $< D^{3D}_{sky}(T) >_{T\to 0\ K} \approx D^{\ 0}_{0\ sky}\left(1 + \frac{k_B T}{a_0\left(D^{\ 0}_{0\,sky}\right)^2}\right)$ [13], while that of $\sigma^{2D}_{<D^{2D}_{sky}>}(T)_{(T\to 0\,K)}$ is exactly superimposed to that of $\sigma^{3D}_{<D^{3D}_{sky}>}(T)_{(T\to 0\,K)}$ because $\sigma^{2D}_{<D^{2D}_{sky}>(T\to 0\,K)} = \sigma^{3D}_{<D^{3D}_{sky}>(T\to 0\,K)}$. Instead, as occurs at higher temperatures, S^{2D} is consistently downshifted with respect to S^{3D}. Since these numerical calculations do not add further physical information to the discussion, they are not shown in Section 3.

3. Results and Discussion

In this section, the main results of this work applied to an outwardly Néel skyrmion hosted in a Co dot of radius R_d = 200 nm and t = 0.8 nm having the core magnetization m_z (r = 0) = −1 (S = −1) and $\mathbf{H}_{ext}$ applied along + z are discussed. The magnetic parameters are the ones used in the analytical and numerical calculations in [13,14]. In particular, the following magnetic parameters at T = 0 K were used: saturation magnetization M_s = 600 KA/m, exchange stiffness constant A = 20 pJ/m, IDMI parameter D = 3.0 mJ/m^2, K_u = 0.6 MJ/m^3 (for example, Co). The magnetic parameters A, D and K_u at non-zero temperature are scaled from their zero temperature values, by using the scaling laws $A(m) = A$ (T = 0 K) m $(T)^{3/2}$, D $(T) = D(T = 0$ K) $m(T)^{3/2}$, and K_u $(T) = K_u$ (T = 0 K) $m(T)^{3.6}$ [15]. In Table 1 are summarized the values of a and of D_{0sky} used in the numerical calculations [13,14]. Table 1 does not contain the values of a and D_{0sky} at T = 0 K since the shown calculations are for $T \geq 50$ K.

Table 1. Calculated a and $D_{0\ sky}$ used in the numerical calculations [13,14].

T (K)	a (×10^{-5} J/m^2) μ_0H = 0 mT	D_{0sky} (nm) μ_0H = 0 mT	a (×10^{-5} J/m^2) μ_0H = 25 mT	D_{0sky} (nm) μ_0H = 25 mT	a (×10^{-5} J/m^2) μ_0H = 50 mT	D_{0sky} (nm) μ_0H = 50 mT
50	6.42	30.83	11.15	24.42	15.03	21.22
100	5.15	34.43	9.67	26.83	13.85	22.42
150	3.86	39.64	8.46	29.23	12.57	24.02
200	2.69	46.85	7.33	32.03	11.28	26.03
250	1.62	58.46	6.33	35.24	10.04	28.43
300	0.71	81.28	5.32	39.64	9.02	30.83

In Figure 2, the 2D skyrmion diameters distribution calculated via Equation (2) (solid black lines) is compared to the 3D distribution (dashed red lines) [13] obtained by means of Equation (1) for three different temperatures, T = 100 K, 200 K and 300 K, respectively and, at fixed T, for three values of the external bias field, μ_0 H_{ext} = 0 mT, 25 mT and 50 mT, respectively.

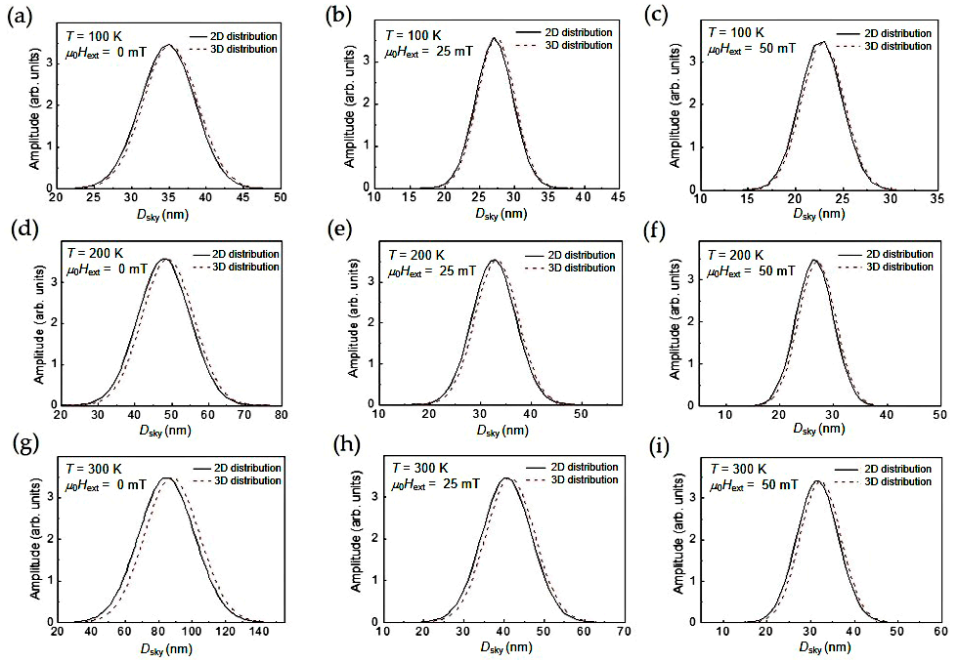

Figure 2. Comparisons between the 2D (solid black lines) and 3D (dashed red lines) skyrmion diameters distributions at: (**a**) T = 100 K and μ_0H_{ext} = 0 mT; (**b**) T = 100 K and μ_0H_{ext} = 25 mT; (**c**) T = 100 K and μ_0H_{ext} = 50 mT; (**d**) T = 200 K and μ_0H_{ext} = 0 mT; (**e**) T = 200 K and μ_0H_{ext} = 25 mT; (**f**) T = 200 K and μ_0H_{ext} = 50 mT; (**g**) T = 300 K and μ_0H_{ext} = 0 mT; (**h**) T = 300 K and μ_0H_{ext} = 25 mT; (**i**) T = 300 K and μ_0H_{ext} = 50 mT. (The 3D skyrmion diameters distributions at T = 100 K, 200 K and 300 K and μ_0H_{ext} = 25 mT are the analytical distributions shown in Figure 3 of [13]).

One notes that the 2D and 3D distributions are almost superimposed at low temperature (T = 100 K) for any amplitudes of the external bias field, while at higher temperatures (T = 200 K, 300 K) there is a shift of the 3D distribution towards higher values together with a broadening of the distribution itself marked by an increase of the full width at half maximum (FWHM). The shift and the broadening of the 3D distributions are attenuated with increasing the amplitude of the external bias field. Therefore, H_{ext} partially masks the effect due to the increase of the dimensionality on the skyrmion diameters distribution.

The displacement of the maximum passing from the 2D to the 3D skyrmions distribution shown in Figure 2 is highlighted in Figure 3 displaying the most probable skyrmion diameters of the 2D and 3D distributions. The calculation of the most probable diameters for the 2D (3D) case was performed according to Equation (4) (Equation (3)). The general trend is a monotonic increase of the most probable diameter vs. T according to both approaches with a strong deviation from linearity for $T > 200$ K and especially in the absence of an external field. However, while for $T < 150$ K the most probable diameters of the 2D and 3D distributions are almost superimposed, at higher temperatures $D_{sky}^{mp\ 3D}$ values are larger than $D_{sky}^{mp\ 2D}$ ones especially in the absence of an external bias field.

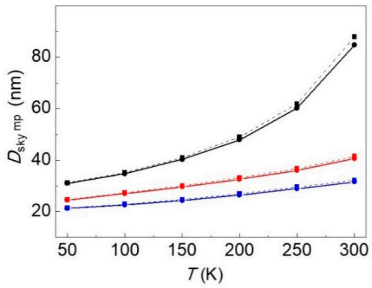

Figure 3. 2D (solid lines) and 3D (dashed lines) most probable skyrmion diameters as a function of T for $\mu_0 H_{ext}$ = 0 mT (black lines); $\mu_0 H_{ext}$ = 25 mT (red lines) and $\mu_0 H_{ext}$ = 50 mT (blue lines).

Similar conclusions can be drawn from the comparison of $< D_{sky}^{3D} >$ and $< D_{sky}^{2D} >$ vs. T for the 2D and 3D distributions calculated by means of Equations (6) and (7), respectively as illustrated in Figure 4a (note that the numerical values of $< D_{sky}^{3D} >$ and $< D_{sky}^{2D} >$ are not coincident with those of $D_{sky}^{mp\ 3D}$ and $D_{sky}^{mp\ 2D}$, respectively but are very close to them).

Instead, the broadening of the distributions of the skyrmion diameters is highlighted in Figure 4b that shows the comparison between $\sigma^{2D}_{<D_{sky}>}(T)$ (continuous line) calculated by means of Equation (9) and $\sigma^{3D}_{<D_{sky}>}(T)$ (dashed lines) obtained via Equation (10). The general trend of the standard deviation is a monotonic increase as a function of T with a deviation from the linear behavior especially in the absence of an external bias field. It is evident that, especially in the range 200 K $\leq T \leq$ 300 K, $\sigma^{3D}_{<D_{sky}>}(T)$ has higher values confirming the broadening of the distributions passing from a 2D to a 3D model marked by the increase of the FWHM.

In Figure 5a the configurational entropy vs. T calculated within the 2D model (continuous lines) according to Equation (15) is compared to the one determined within the 3D model (dashed lines) by means of Equation (16) using the values of a and D_{0sky} summarized in Table 1 and Equations (6) and (7), respectively. The increasing monotonic trend as a function of T of the configurational entropy is similar in the two cases becoming more pronounced in the absence of an external magnetic field and especially within the 3D model. The increase of the configurational entropy with increasing T marks the increase of the disorder due to the temperature that is enhanced within a 3D description. This disorder is partially attenuated by the perturbation effect of an external applied field and this is confirmed also by the results of the 2D model. However, within the 2D model the curves of S^{2D} in the presence of an applied field are almost superimposed showing that the perturbation effect on the configurational entropy of the external bias field is weaker with respect to that occurring within the

3D model. Remarkably, the passage from a 3D to a 2D description leads to a consistent lowering of the configurational entropy that in the 2D model is almost one order of magnitude less than in the 3D model. This occurs also in the presence of an external bias field. The reason of this quantitative difference can be attributed to the different power dependence on the temperature T and to the key role played by the skyrmion thickness in the 3D description as inferred comparing Equation (15) with Equation (16). Figure 5b shows the comparison between the calculated 2D and 3D configurational entropy, S^{2D} and S^{3D}, respectively as a function of the external bias field at fixed T for T = 300 K. While the ordering effect of the external bias field is rather pronounced in the 3D model, as evidenced by the reduction of the configurational entropy with increasing the external magnetic field, in the 2D model, surprisingly the configurational entropy exhibits a minimum and, for $\mu_0 H_{ext} > 50$ mT, increases breaking the typical decreasing monotonic behavior with increasing H_{ext} that marks the ordering effect of the external magnetic field. The breaking of the monotonic behavior occurs also at other temperatures (not shown). This effect on S^{2D} could be only numerical taking into account that S^{2D} is approximated because its calculation is based on the skyrmion energy harmonic approximation. Therefore, it could depend on some numerical errors arising from the approximation of the real skyrmion energy that are enhanced with increasing the amplitude of the external bias field and that can result more effective in the calculation of S^{2D}. Actually, a simple physical consideration can be done. For this type of thermodynamic systems the entropic contribution TS to the Helmholtz free energy $F = \langle E \rangle - T\,S$, with $\langle E \rangle \approx a \langle D_{sky}{}^2 \rangle$ the average skyrmion energy, should be of the same order of $\langle E \rangle$ (on average about 10^{-20} J) resulting in F at least one order of magnitude less than each of the energetic and entropic contributions. Nevertheless, this occurs only within the 3D description. Finally, note that the 3D description was also supported by micromagnetic simulations that accounted for the thickness t of the ferromagnetic material [13]. According to those considerations, one concludes that, albeit skyrmions are planar structures, a 3D theoretical description to discuss the statistical thermodynamic properties including also a dependence on the thickness t of the magnetic skyrmion is preferable. A final confirmation of which of the two descriptions is the more realistic one could come, for example, from calorimetric measurements able to determine in an accurate way the entropy of a magnetic skyrmions population.

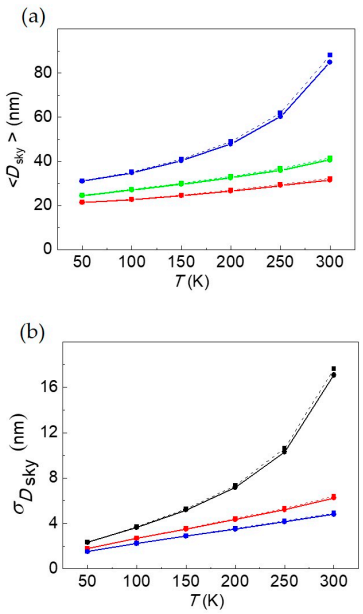

Figure 4. (**a**) 2D (solid lines) and 3D (from Table 1 of [14]) (dashed lines) average skyrmion diameters as a function of T for $\mu_0 H_{ext}$ = 0 mT (blue lines); $\mu_0 H_{ext}$ = 25 mT (green lines) and $\mu_0 H_{ext}$ = 50 mT (red lines); (**b**) standard deviation of the 2D (continuous lines) and 3D (dashed lines) distribution (from Figure 4 of [13]) as a function of T for $\mu_0 H_{ext}$ = 0 mT (black lines); $\mu_0 H_{ext}$ = 25 mT (red lines) and $\mu_0 H_{ext}$ = 50 mT (blue lines).

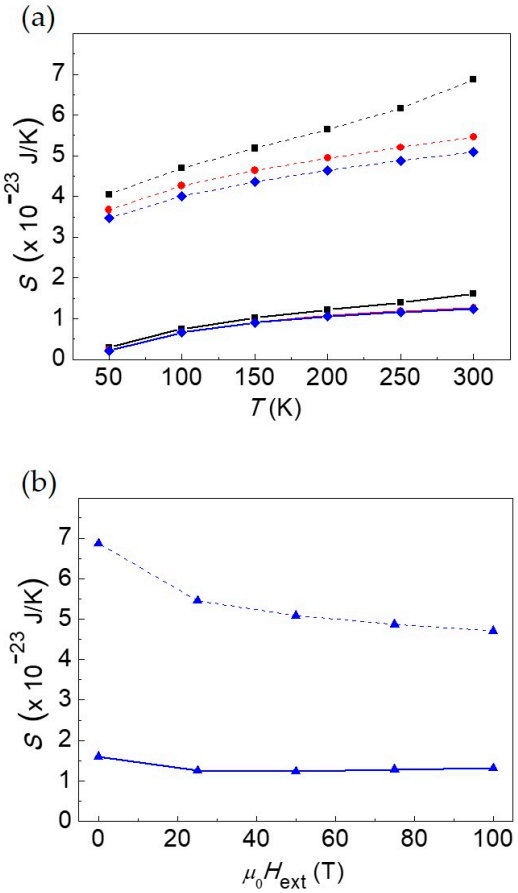

Figure 5. (**a**) Configurational entropy as a function of T for a 2D skyrmions distribution (solid lines) and for a 3D skyrmions distribution (from Figure 5 of [13]) (dashed lines) for $\mu_0 H_{\text{ext}}$ = 0 mT (black lines); $\mu_0 H_{\text{ext}}$ = 25 mT (red lines) and $\mu_0 H_{\text{ext}}$ = 50 mT (blue lines); (**b**) configurational entropy as a function of the external bias field at T = 300 K for a 2D and for a 3D skyrmions population distribution (from Figure 5 of [13]). The meaning of the blue lines (solid and dashed) is the same as in panel (**a**). For the calculation of S^{2D} at $\mu_0 H_{\text{ext}}$ = 75 mT ($\mu_0 H_{\text{ext}}$ = 100 mT) the following parameters were used: $a = 12.45 \times 10^{-5}$ J/m^2 ($a = 15.71 \times 10^{-5}$ J/m^2) and $D_{0\text{sky}}$ = 25.87 nm ($D_{0\text{sky}}$ = 22.51 nm).

4. Statistical Thermodynamic Entropy and Information Entropy

In this section, firstly the close resemblance of Boltzmann's statistical thermodynamic entropy definition at equilibrium used to calculate the configurational entropy for a 2D skyrmions population with information entropy [16–26] is discussed. Secondly, a qualitative description that can be used for a possible future application is given.

Let us define a discrete random variable X = $\{x_1, x_2, \ldots x_N\}$ where x_i are its possible values. According to Shannon's definition in information theory [18,19], the information entropy written in compact form is the dimensionless quantity $H(X) = E(I(X))$. Specifically, $E(I(X))$ is the expectation value of I(X) with $I(X) = -\log_b(P(X)) = \log_b(1/P(X))$ the information content (otherwise called "surprisal"), being b the basis of the logarithm and $0 \leq P(X) \leq 1$ the probability mass function or discrete density function giving the probability that the discrete random variable X is exactly equal to some value. In explicit form, the information entropy written, for example, in units of bits, b = 2 with $\log_2 2 = 1$ bit, takes the form $H(X) = -\sum_{i=1}^{N} P(x_i) \log_2(P(x_i))$ where $-\log_2(P(x_i))$ is the information content associated to the value x_i having probability $P(x_i)$. Hence, the information entropy can be regarded as the average value E of the information or information content produced by a stochastic source of data measuring the unpredictability of the state. The more the probability is lower, the more the information content is higher and the more the information entropy is higher.

Similarly, because of the strict analogy between information and physics [20,21] and, more specifically, between information and statistical mechanics [22,23], Boltzmann's statistical thermodynamic entropy at equilibrium $S = -k_B <\ln f_0>$ is proportional to the equilibrium Boltzmann order function $H_0 = <\ln f_0>$ that is expressed as the statistical average of $\ln f_0$ (Equations (11) and (12)), being f_0 the Gaussian probability distribution.

According to the above definitions, both the information and the statistical thermodynamic entropy are non-negative quantities. Therefore, entropy is a measure of disorder or uncertainty in information theory as in statistical thermodynamics. However, note that, within the present analytical framework, S is calculated in the continuous limit while Shannon's entropy is calculated in the discrete case. This means that there is only an analogy between the two definitions but not a complete identification. To get a complete identification of Boltzmann's statistical thermodynamic entropy at equilibrium with Shannon's entropy one should consider the recently obtained micromagnetic results whose simulated Néel skyrmion distributions of diameters are discrete (see e.g., [13,15]). Instead, the statistical configurational entropy calculated analytically has a complete identification with Jaynes's continuous information entropy based on the concept of the limiting density of a set of discrete points [24–26]. Jaynes's definition of information entropy is the correct continuous limit of discrete Shannon's information entropy. Indeed, continuous Shannon's information entropy, otherwise called differential entropy, suffers from the limitations that it can assume also negative values, is not invariant under a change of variable and is not dimensionally correct. Jaynes's continuous information entropy can be written in the dimensionless form for the one-dimensional case as:

$$H(X) = -\int_X p(x) \log_2\left(\frac{p(x)}{m(x)}\right) dx \tag{20}$$

where $p(x)$ is the probability density function referred to the continuous variable x and the function $m(x)$, called the "invariant measure", makes part of the definition of the limit of the density of a set of N discrete points $\{x_i\}$ as $N \to \infty$ such that $\lim_{N\to\infty} \frac{1}{N} = \int_a^b m(x)\, dx$ with a and b the extremes of the interval of integration. Both $p(x)$ and $m(x)$ have the dimension of the inverse of a length to make H(X) dimensionless.

The key message contained in Shannon's information entropy and in its continuous Jaynes's version (Equation (20)) is the following: a low-probability event carries more information than a high probability event. In other words, if an event is less probable, due to its high degree of unpredictability, is more interesting than a high-probability event.

If this concept is transferred to the configurational statistical entropy of a skyrmion diameters population, the information is contained in $\ln f_0$ regarded as a Gaussian probability distribution appearing in the expression of the equilibrium Boltzmann order function (Equations (11) and (12)). As for the case of Shannon's and Jaynes's information entropy, the amount of information carried out by each of the different events is a random variable represented by the skyrmion size at a given T and instant of time whose expectation value is the information entropy determined at each temperature. Let us suppose having a distribution of skyrmion diameters obtained taking pictures of the skyrmions at different instants of time having the same average energy, as observed in micromagnetic simulations [13], no matter if it is analytically modelled via a 2D or 3D distribution. The event (message) occurring at the instant of time t_1 when the skyrmion area is ${A_{sky}}^{mp} = \frac{1}{4}\pi\,({D_{sky}}^{mp})^2$ corresponding to the most probable skyrmion diameter carries less information than all the events occurring in different instants of time corresponding to skyrmion diameters D_{sky} such that $A_{sky} \neq {A_{sky}}^{mp}$. Taking into account the information entropy concept, the more D_{sky} is far away from ${D_{sky}}^{mp}$, the less is its probability and the more the corresponding event carries information. In other words, the more the area A_{sky} differs from ${A_{sky}}^{mp}$, the more the event is unpredictable and the more it encodes information. It has been found that the effect of temperature is the broadening of the distributions of the skyrmion diameters at every

external bias field (see Figure 2). With increasing temperature the interval of diameters belonging to the distribution increases leading to a higher number of events carrying more information and to a higher entropy encapsulating more information (see Figure 5a). On the other hand, the effect of the external bias field is opposite: at fixed temperature there is the narrowing of the distributions of diameters with increasing H_{ext} leading to a lower number of events carrying more information and to a lower entropy encapsulating less information (see Figure 5b). Hence, via the analogy between Shannon's and Jaynes's entropy and the configurational thermodynamic entropy, the following arguments have been demonstrated: (1) room temperature magnetic skyrmions carry more information entropy than the ones at low temperature; (2) at fixed temperature, in the region of metastability, magnetic skyrmions that are not perturbed by an external bias field encapsulate more information entropy than the ones subject to H_{ext}. These conclusions could be drawn already looking at Figure 5 but only within a statistical thermodynamic framework.

Finally, a simple example of entropy data communication system using ferromagnetic materials hosting magnetic skyrmions is suggested. In information theory for data communication systems one should distinguish among: (1) a data source, (2) a communication channel and (3) a receiver. The receiver should interpret the data that come from the source observing and collecting them. For the ferromagnetic system studied, the data source of entropy information can be regarded as a thermal bath at a given T in contact with the ferromagnetic material (e.g., cylindrical dot) hosting the magnetic skyrmion exciting the thermal breathing mode that acts as a source of entropy. The communication channel can be thought of the ferromagnetic material itself where the magnetic skyrmion forms that is able to collect the entropy information bits coming from the magnetic skyrmion. The receiver could be a special device able to identify and collect the bits of entropy. It can be ideally supposed that the amount of entropy is less than the capacity of the communication channel leading to the communication of all the data to the receiver.

5. Conclusions

In summary, it has been shown that it is possible to determine the statistical properties and the configurational entropy related to the size changes of a population of magnetic skyrmions according to a 2D model basing on the fact that magnetic skyrmions are planar structures. The analogy with the 3D MB distribution for the ideal gas is not anymore so stringent as occurred within the 3D model of a population of skyrmions but it can still be applied, without loss of generality, in the region of skyrmion metastability studied in this work. The analysis was carried out discussing the comparison of the results obtained according to the 2D model with the ones derived within the 3D model. It has been shown that both the 2D and 3D models lead to similar quantitative results related to skyrmions distribution statistical properties such as the skyrmion average size as a function of the temperature. Instead, some quantitative discrepancies regarding the configurational entropy calculation have been found being S^{2D} almost one order of magnitude less than S^{3D}. These discrepancies are not surprising because the two models lead to a different power dependence of S^{2D} and S^{3D} on the thermal energy. In addition, within the 3D description, there is also an explicit dependence on the thickness of the ferromagnetic material that gives a further contribution to the entropy. According to some physical arguments related to the estimation of the average energy and the entropy contribution to the Helmholtz free energy that should be comparable in a thermodynamic system such as the one studied, and taking into account some micromagnetic observations, the results regarding the thermodynamic properties of the 3D model are preferable. However, a final confirmation could come from the measurement of the entropy and the heat exchanged using, for example, calorimetric techniques.

Finally, a qualitative description of an entropy data communication system has been given for a future possible application of magnetic skyrmions as temperature and magnetic field dependent information entropy carriers. This was proposed exploiting the strong analogy between Boltzmann's statistical entropy and Jaynes continuous version of Shannon's information entropy. It has been shown that the magnetic skyrmion at room temperature carries more entropy information than at low

temperature and that, under an external bias field, at fixed temperature the encapsulated information entropy reduces with increasing the magnetic field amplitude.

Funding: This research received no external funding.

Acknowledgments: The author acknowledges support by Gruppo Nazionale per la Fisica Matematica (GNFM) and Istituto Nazionale di Alta Matematica (INdAM) "F. Severi." The author wish to give a special thanks to Riccardo Tomasello and Giovanni Finocchio for fruitful discussions.

Conflicts of Interest: The author declares no conflict of interest.

References

1. Fert, A.; Cros, V.; Sampaio, J. Skyrmions on the track. *Nat. Nanotechnol.* **2013**, *8*, 152–156. [CrossRef] [PubMed]
2. Fert, A.; Reyren, N.; Cros, V. Magnetic skyrmions: Advances in physics and potential applications. *Nat. Rev. Mater.* **2017**, *2*, 17031. [CrossRef]
3. Dzyaloshinskii, I. A thermodynamic theory of 'weak' ferromagnetism of antiferromagnetics. *J. Phys. Chem. Solids* **1958**, *4*, 241–255. [CrossRef]
4. Moriya, T. Anisotropic superexchange interaction and weak ferromagnetism. *Phys. Rev.* **1960**, *120*, 91–98. [CrossRef]
5. Bogdanov, A.N.; Rossler, U.K. Chiral symmetry breaking in magnetic thin films and multilayers. *Phys. Rev. Lett.* **2001**, *87*, 037203. [CrossRef]
6. Rößler, U.K.; Bogdanov, A.N.; Pfleiderer, C. Spontaneous skyrmion ground states in magnetic metals. *Nature* **2006**, *442*, 797. [CrossRef]
7. Guslienko, K.Y. Skyrmion State Stability in Magnetic Nanodots with Perpendicular Anisotropy. *IEEE Magn. Lett.* **2015**, *6*, 4000104. [CrossRef]
8. Tomasello, R.; Giordano, A.; Chiappini, S.; Zivieri, R.; Siracusano, G.; Puliafito, V.; Medlej, I.; La Corte, A.; Azzerboni, B.; Carpentieri, M.; et al. Micromagnetic understanding of the skyrmion Hall angle current dependence in perpendicularly magnetized ferromagnets. *Phys. Rev. B* **2018**, *98*, 224418. [CrossRef]
9. McKeever, B.F.; Rodrigues, D.R.; Pinna, D.; Abanov, A.; Sinova, J.; Everschor-Sitte, K. Characterizing breathing dynamics of magnetic skyrmions and antiskyrmions within the Hamiltonian formalism. *Phys. Rev. B* **2019**, *99*, 054430. [CrossRef]
10. Ge, M.; Zhang, L.; Menzel, D.; Han, H.; Jin, C.; Zhang, C.; Pi, L.; Zhang, Y. Scaling investigation of the magnetic entropy change in helimagnet MnSi. *J. Alloys Compd.* **2015**, *649*, 46–49. [CrossRef]
11. Han, H.; Menzel, D.; Liu, W.; Ling, L.; Du, H.; Pi, L.; Zhang, C.; Zhang, L.; Zhang, Y. Scaling of the magnetic entropy change in skyrmion material $Fe_{0.5}Co_{0.5}$ Si. *Mater. Res. Bull.* **2017**, *94*, 500. [CrossRef]
12. Wild, J.; Meier, T.N.G.; Pöllath, S.; Kronseder, M.; Bauer, A.; Chacon, A.; Halder, M.; Schowalter, M.; Rosenauer, A.; Zweck, J.; et al. Entropy-limited topological protection of skyrmions. *Sci. Adv.* **2017**, *3*, e1701704. [CrossRef] [PubMed]
13. Zivieri, R.; Tomasello, R.; Chubykalo-Fesenko, O.; Tiberkevich, V.; Carpentieri, M.; Finocchio, G. Configurational entropy of magnetic skyrmions as an ideal gas. *Phys. Rev. B* **2019**, *99*, 174440. [CrossRef]
14. Zivieri, R. Statistical Thermodynamics of Chiral Skyrmions in a Ferromagnetic Material. *Materials* **2019**, *12*, 3702. [CrossRef] [PubMed]
15. Tomasello, R.; Guslienko, K.Y.; Ricci, M.; Giordano, A.; Barker, J.; Carpentieri, M.; Chubykalo-Fesenko, O.; Finocchio, G. Origin of temperature and field dependence of magnetic skyrmion size in ultrathin nanodots. *Phys. Rev. B* **2018**, *97*, 060402. [CrossRef]
16. Pathria, R.K.; Beale, P. *Statistical Mechanics*, 3rd ed.; Academic Press: Cambridge, MA, USA, 2011; p. 51.
17. Jones, D.S. *Elementary Information Theory*; Clarendon Press: Oxford, UK, 1979.
18. Shannon, C.E. A Mathematical Theory of Communication. *Bell Syst. Tech. J.* **1948**, *27*, 379–423. [CrossRef]
19. Shannon, C.E.; Weaver, W. *The Mathematical Theory of Communication*; University of Illinois Press: Urbana, IL, USA, 1949.
20. Landauer, R. Information is physical. *Phys. Today* **1991**, 23–29. [CrossRef]
21. Landauer, R. The physical nature of information. *Phys. Lett. A* **1996**, *217*, 188. [CrossRef]
22. Jaynes, E.T. Information Theory and Statistical Mechanics I. *Phys. Rev.* **1957**, *106*, 620–630. [CrossRef]

23. Jaynes, E.T. Information Theory and Statistical Mechanics II. *Phys. Rev.* **1957**, *108*, 171–190. [CrossRef]
24. Jaynes, E.T. Information Theory and Statistical Mechanics. In *Statistical Physics*; Ford, K., Ed.; Benjamin: New York, NY, USA, 1963; p. 181.
25. Jaynes, E.T. Prior Probabilities. *IEEE Trans. Syst. Sci. Cybern.* **1968**, *SSC-4*, 227. [CrossRef]
26. Jaynes, E.T. *Probability Theory: The Logic of Science*; Cambridge University Press: New York, NY, USA, 2003.
27. Bazeia, D.; Moreira, D.C.; Rodrigues, E.I.B. Configurational entropy for skyrmion-like magnetic structures. *J. Magn. Magn. Mater.* **2019**, *475*, 734. [CrossRef]
28. Gleiser, M.; Stamatopoulos, N. Entropic measure for localized energy configurations: Kinks, bounces, and bubbles. *Phys. Lett. B* **2012**, *713*, 304–307. [CrossRef]
29. Müller, J. Magnetic skyrmions on a two-lane racetrack. *New J. Phys.* **2017**, *19*, 025002. [CrossRef]
30. Chui, C.; Zhou, Y.; Liu, W.; Xu, Y. Magnetic skyrmions as information carriers. *Lowl. Technol. Int.* **2017**, 16–21.
31. Kang, W.; Chen, X.; Zhu, D.; Li, S.; Huang, Y.; Zhang, Y.; Zhao, W. Magnetic skyrmions for future potential memory and logic applications: Alternative information carriers. In Proceedings of the 2018 Design, Automation & Test in Europe Conference & Exhibition (DATE), Dresden, Germany, 19–23 March 2018. [CrossRef]
32. Zhou, Y.; Ezawa, M. A reversible conversion between a skyrmion and a domain wall pair in a junction geometry. *Nat. Comm.* **2014**, *5*, 4652. [CrossRef]